A Method for Characterizing Effective Pore Sizes of Catalysts

Charles Edwin Webster,* Russell S. Drago,† and Michael C. Zerner

Center for Catalysis, Department of Chemistry, University of Florida, Gainesville, Florida 32611

Received: October 13, 1998

The temperature dependent effective catalytic pore size can be determined by the comparison of ^{13}C MAS NMR spectra of heterogeneously catalyzed, shape selective reactions and data collected from GC analysis of the product stream of reactions under similar reaction conditions. The concept of effective minimum molecular dimensions has been set forth in a previous paper. (Webster, C. E.; Drago, R. S.; Zerner, M. C. *J. Am. Chem. Soc.* **1998**, *120*, 5509−5516.) In this investigation, it is concluded that the effective catalytic channel size of HZSM-5 is between 6.62 and 7.27 Å at 300 °C, the MIN-2 dimensions of *p*-xylene and *o*-xylene, respectively. At 370 °C, the effective catalytic channel size is increased to a minimum of 7.64 Å, the MIN-2 dimension of 1,2,3-trimethylbenzene. We discuss the apparent increase in the effective catalytic channel intersection size with increasing temperature. This novel approach presents an a priori description of relative pore sizes and can be used to investigate and describe numerous catalytic and adsorbent systems as discussed in this paper. The comparison of observed isomer distributions of the trimethylbenzenes to their thermodynamic equilibrium distributions provides experimental evidence for the existence of the previously reported nest effect, which describes the shape selectivity of the exterior surface of the HZSM-5 structure.

Introduction

Zeolites have played a major role in shape and size selective catalysis. The properties of these heterogeneous catalysts and other solid adsorbents have been widely studied and discussed.[1−3] The selectivity of these structures has been a major concern since the first use of zeolite Y as an isomerization catalyst in 1959.[4] The zeolite's inherent control over a reaction within the internal constraints of the structure directs this selectivity at the molecular level. Selectivity in heterogeneously catalyzed reactions arises from reactant selectivity, two types of product selectivity, and restricted transition-state selectivity.

Reactant selectivity is a case in which potential reactants are excluded based upon their size compared to that of the pore dimensions. Different zeolites have distinct window openings to their channel system. There are more than 50 different available aluminosilicate zeolites with pore openings ranging from less than 5 Å to larger than 10 Å,[5] and silicoaluminophosphates extend this upper limit to 13 Å.[6] This selectivity and a wide number of zeolites give the potential to preferentially use certain reactants in a catalytic reaction within a multiple reactant system. Many examples of this type of selectivity are found in the literature.[5] A simple diagrammatic representation of reactant selectivity is shown in Figure 1a.

Product selectivity may be obtained by two different means: preferential diffusion and size exclusion. Preferential-diffusion product selectivity appears when two or more reaction products made within the confines of the structure have apparent diffusivities, which sufficiently differ to allow one product to preferentially diffuse out of the structure. Often, the smaller diffusivity of the larger isomer allows for isomerization to the diffusion preferred (smaller) product. One must recall that a reaction product is a molecule formed within the structure by the reaction, but that not all reaction products necessarily appear in the product stream. Preferential-diffusion product selectivity, which has been referred to as configurational diffusion controlled selectivity,[9] is represented in Figure lb.

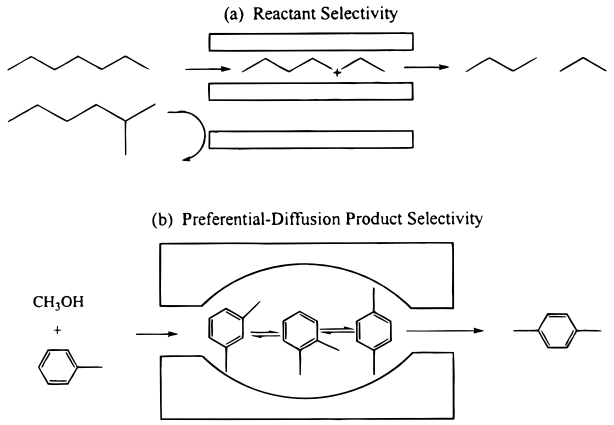

Figure 1. (a) Representation of reactant shape selectivity in zeolite channels (rejection of branched chain hydrocarbons). After ref 7. (b) Representation of preferential-diffusion product shape selectivity (*p*-xylene diffuses preferentially out of the channels). After ref 8.

The second type of product selectivity, size-exclusion, arises from an actual confinement of a reaction product within the structure of the solid. Exclusion product selectivity had been hypothesized, and the work of Anderson and Klinowski[10] demonstrated the experimental evidence. This type of selectivity is represented in Figure 2a.

The final type of selectivity to be discussed is restricted transition-state selectivity. For this type of selectivity, certain types of transition states are too large to be contained within the pores (or, if present, intersections) of the structure. Experimental evidence for transition-state selectivity comes from low temperature cyclization of dienes inside H-mordenite (H-MOR, a large pore zeolite) and HZSM-5 (a medium pore zeolite.)

* To whom correspondence should be addressed. Phone: (352) 392-5263. Fax: (352) 392-4658.

† Deceased. December 5, 1997.

10.1021/jp984055n CCC: $18.00
Published on Web 02/09/1999

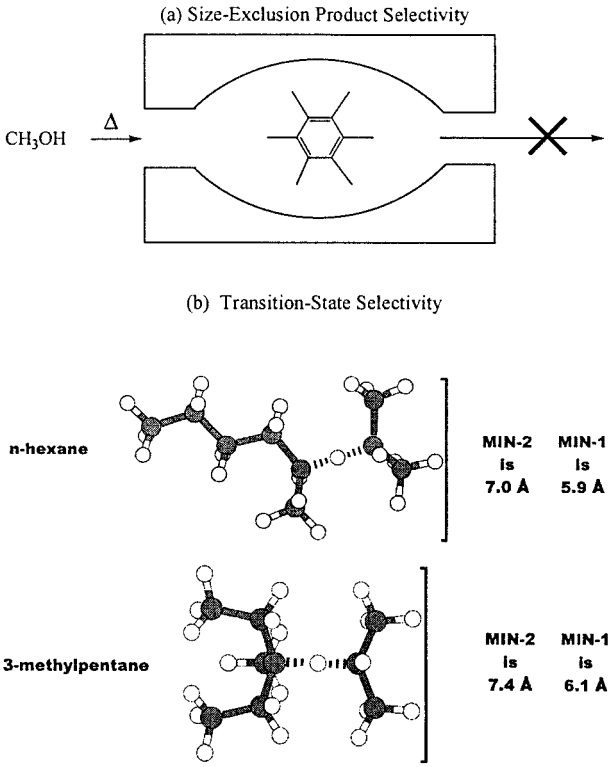

Figure 2. (a) Representation of size-exclusion shape selectivity (hexamethylbenzene cannot diffuse out of the intersection). (b) 3-Methylpentane is a bulkier molecule than *n*-hexane, therefore its transition state has a larger cross section. The transition states and their sizes were calculated using ZINDO.[20]

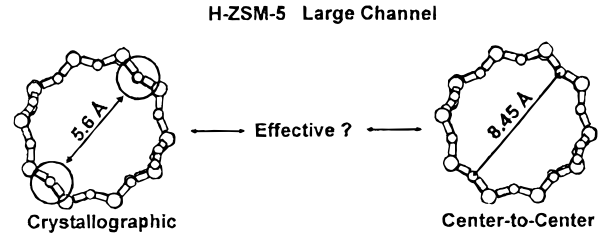

Figure 3. Crystallographic pore size versus center-to-center distance. Crystallographic pore size based on oxygen atom radius of 1.35 Å. The values used for the center-to-center oxygen distances were obtained from the fractional coordinates of the van Koningsveld et al. (*Acta. Crystallogr.* **1987**, *B43*, 127−132) which had improved framework accuracy over previous reports. The oxygen atoms used were those chosen by Olson et al.;[11] for the straight channel, the largest (8.449 Å) and smallest (7.922 Å) center-to-center oxygen atom distances give rise to 5.75 Å by 5.22 Å dimensions of the large channel based on an oxygen atom radius of 1.35 Å.

Using electron paramagnetic resonance (EPR) spectroscopy, one can observe the formation of cycloolefinic radical species inside the structure of H-MOR compared to HZSM-5 where no cycloolefinic radicals are formed.[8] Figure 2b is a representation of different sized transition states. In this case, 3-methylpentane has a bulkier transition state than does *n*-hexane (determined by calculated minimum dimensions).

To date, the investigation and subsequent reporting of the effective pore size of zeolite catalysts has not been systematic with respect to the reactions catalyzed by a particular solid. The literature values, determined from crystallographic measurements, for the window size of the straight (large) channel of HZSM-5 are 5.6 Å by 5.4 Å and for the zigzag (small) channel of HZSM-5 are 5.5 Å by 5.1 Å.[11] Figure 3 is a representation of the crystallographically determined pore size compared to the oxygen atom center-to-center distances of the large channel of HZSM-5. While these quoted aperture sizes are used throughout the literature, it is well-known that large aromatic molecules (>7 Å) are readily formed in catalytic reactions involving these materials and are found in the product stream at mild reaction conditions (i.e., 300 °C and atmospheric pressure).[12]

Many authors ascribe this discrepancy between reported crystallographic pore sizes of zeolites and catalytic reaction products to thermal vibrations as well as the distortion of the crystal lattice and the adsorbate molecule. This "movement" is said to account for changes of 0.4 Å in the oxygen window sizes.[13]

The early studies of Barrer first noted this discrepancy.[14] Csicsery concluded from the selective disproportionation of ethyltoluene over H-MOR that the effective pore dimensions were somewhere between 8.2 and 8.6 Å.[15] These dimensions are 1.2−1.6 Å greater than the largest dimension of the reported crystallographic measurements (6.7 Å by 7.0 Å). Dwyer et al. determined an elliptical catalytic pore size for HZSM-5 of approximately 5.5 Å by 7 Å on the basis of dewaxing of distillate charge stocks and noted that HZSM-5 can discriminate both molecular size and shape.[16] This report also concluded that H-MOR has a "catalytic pore size" between 9 and 10 Å and ZSM-23 (crystallographic: 4.5 Å by 5.6 Å) has a catalytic pore size of 4.5 Å by 6.5 Å.[16]

Many studies have been conducted on the attractive and repulsive interactions between molecules and solids. A commonly used potential for studying these interactions is the Lennard-Jones (LJ) 12-6 potential, which has several assumptions. The main premise is that a spherically symmetric potential is assumed with an r^{-6} dependence on attractive forces and an r^{-12} dependence on repulsive forces. The minimum allowed separation (σ_{sep}) of two approaching species can be calculated from the LJ 12-6 potential and the equilibrium position (r_{sep}) with eq 1.

$$\sigma_{sep} = 2^{1/6} r_{sep} \quad (1)$$

This equation may be applied to calculate the minimum approachable distance for any system that follows an r^{-12} dependence on repulsive forces. Most systems are well defined by an r^{-12} dependence though r^{-9} to r^{-15} has been used—the "harder" the molecule, the larger the exponent.[17]

Another important consideration in heterogeneously catalyzed reactions is the relationship between exterior shape selectivity and the surface activity of the solid. The shape selectivity of external surface sites of a zeolite has been termed the nest effect.[18] Fraenkel et al. proposed that "half cavities" which contained the acid site were responsible for the selective formation of 2,6- and 2,7-dimethylnaphthalene in the HZSM-5 catalyzed methylation of naphthalene.[19]

Experimental and Calculations

Molecular Dimensions. ZINDO, a series of molecular electronic structure programs from the Quantum Theory Project at the University of Florida,[20] was used to calculate molecular dimensions for both the lowest energy molecular structure and other relevant molecular conformations tabulated in Table 1. Implementation of the subroutine GEPOL (GEometria POLihedro, 1993) calculates the molecular surface area and the molecular volume of a molecule from the calculated structure.[21]

Results and Discussion

Choice of Oxygen Atom Radii. The discrepancy in the literature between pore sizes from refined crystallographic data

TABLE 1: Molecular *x*, *y*, *z*, MIN-1, and MIN-2 Dimensions[a]

molecule	*x* (Å)	*y* (Å)	*z* (Å)	MIN-1 (Å)	MIN-2 (Å)
benzene	6.628	7.337	3.277	3.277	6.628
2,6-di-*tert*-butylpyridine	11.344	6.454	8.294	6.454	8.294
cyclohexane	7.168	6.580	4.982	4.982	6.580
ethylbenzene	6.625	5.285	9.361	5.285	6.625
hexamethylbenzene	9.089	9.079	4.027	4.027	9.079
hexane	10.344	4.536	4.014	4.014	4.536
2,6-lutidine	8.927	4.127	6.957	4.127	6.957
2-methylnaphthalene	10.294	7.354	3.967	3.967	7.354
pentamethylbenzene	9.094	4.029	8.223	4.029	8.223
propylbenzene	6.625	5.277	10.274	5.277	6.625
1,2,3,4-tetramethylbenzene	7.646	4.117	9.099	4.034	7.646
1,2,3,5-tetramethylbenzene	8.549	4.034	9.152	4.034	8.174
1,2,4,5-tetramethylbenzene	7.377	4.034	9.072	4.034	7.377
toluene	6.625	4.012	8.252	4.012	6.625
1,2,3-trimethylbenzene	9.058	4.062	8.227	4.062	7.635
1,2,4-trimethylbenzene	7.576	4.024	9.145	4.024	7.251
1,3,5-trimethylbenzene	8.276	8.553	4.062	4.062	8.178
m-xylene	8.994	3.949	7.314	4.012	7.258
o-xylene	7.269	3.834	7.826	3.834	7.269
p-xylene	6.618	3.810	9.146	3.810	6.618

[a] MIN-1, the minimum dimension through a molecule, and MIN-2, the second minimum dimension through a molecule perpendicular to MIN-1. MIN-1 will determine if the molecule can enter a slit-shaped pore, while MIN-1 and MIN-2 will determine if a molecule can enter a cylindrical pore, Figure 4. Minimum dimensions are meant to be used as a direct comparison of molecular sizes and have no temperature dependence (as do kinetic diameters) and have been determined from calculated molecular structures, which have dimensions shown to correlate well with the bulk density of the molecule[26] (unlike kinetic diameters). See text and ref 26.

and catalytic reaction products is related to the value for the framework oxygen atom radius used to determine the pore window opening. Values of 1.3, 1.35, 1.40, and 1.575 Å have all been used in the zeolite field.[11,22]

With the commonly used value of 1.35 Å, one obtains 5.75 Å by 5.22 Å for the calculated window size of the large channel of HZSM-5.[23] This calculated window size is not large enough to allow for the non-restricted diffusion of *o*-xylene, which is necessary for the 0.0 kcal/mol activation energy for its steady-state diffusion (vide infra).

In fairness, one should also consider the application of the Lennard-Jones (LJ) 12-6 potential to the oxygen radii of the zeolite window. The "minimum radius" of the oxygen atom can be calculated from the relationship of the LJ diameter (σ_{LJ}) and the equilibrium diameter (r_e) by eq 1 assuming a static situation. After this correction is performed for the van der Waals radii of 1.40 Å, the 5.75 Å by 5.22 Å pore size increases to 5.95 Å by 5.43 Å, which is again too small a pore diameter to allow these large aromatics to diffuse in the HZSM-5 structure. If one applies the correction to the O^{2-} radii of 1.32 Å,[25] one obtains a pore size of 6.10 Å by 5.57 Å—still too small.

While the radius of the oxygen atoms of a zeolite could be thought of as a radial distribution function describing the extension of the electron probabilities of the orbitals (increasing the "sponginess" of the oxygen atoms), the unhindered diffusion of the larger aromatic molecules precludes the necessity of such an argument (except for the largest molecules at 370 °C which could possibly have an activation energy for steady-state diffusion). The omission of a discussion of a radial distribution describing the oxygen atom radius does not detract from the validity of such an argument, when found necessary by the experimental conclusions. Larger molecules are allowed to diffuse through a more restricted opening if the oxygen atoms are considered "spongy".

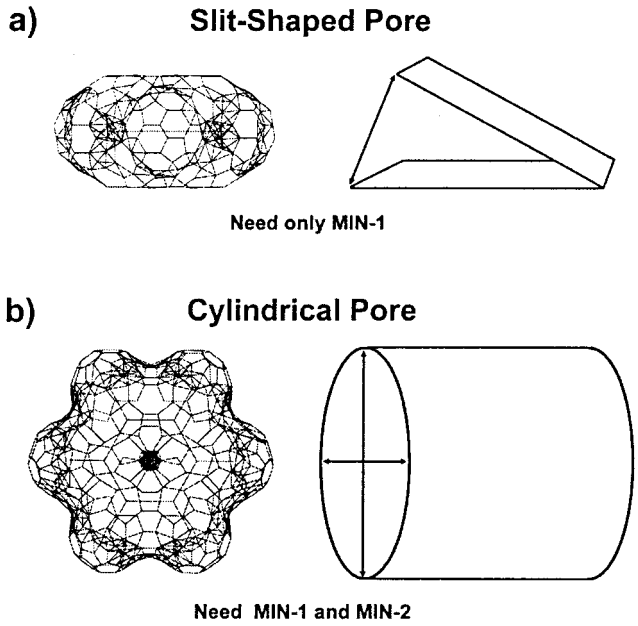

Figure 4. Application of the MIN-1 and MIN-2 of a benzene molecule to pore access. The minimum dimensions of the adsorptive dictate pore access. In (a), MIN-1 less than the dimension of a slit-shaped pore is required for access. In (b), MIN-1 and MIN-2 less than the two dimensions of a cylindrical pore is required for access.

Minimum Dimensions. The concept of effective minimum dimensions of molecules has been set forth in a previous paper.[26] MIN-1, the minimum dimension through a molecule, and MIN-2, the second minimum dimension through a molecule perpendicular to MIN-1, determine whether or not a molecule can enter a pore. MIN-1 will determine if the molecule can enter a slit-shaped pore, while MIN-1 and MIN-2 will determine if a molecule can enter a cylindrical pore (Figure 4).

Minimum dimensions are meant to be used as a direct comparison of molecular sizes and have no temperature dependence (as do kinetic diameters) and have been determined from calculated molecular structures, which have dimensions shown to correlate well with the bulk density of the molecule[26] (unlike kinetic diameters). Minimum dimensions are static descriptors of a dynamic process.

Effective Catalytic Pore Size. The apparent change in size of the HZSM-5 channel and the intersection, realized from a change in temperature, can be determined from the analysis of the ^{13}C MAS NMR spectra of HZSM-5 catalyzed, shape-selective conversion of methanol to gasoline,[10] and data collected from GC analysis of the product stream of the same reaction at two temperatures.[12,27a] The products of this conversion for the two temperatures and the relevant adsorbed specie for the two temperatures are tabulated in Table 2. It should be noted that the intensities quoted in the adsorbed phase are only a rough estimate of their concentration[10] due to the nuclear Overhauser effect (nOe).

At 300 °C, the product stream of the HZSM-5 catalyzed conversion of methanol to higher molecular weight alkanes and aromatics (i.e., gasoline) contains aromatic molecules as large as *m*-xylene (Tables 1 and 2). The next larger aromatic molecules in the adsorbed phase, as determined from the ^{13}C MAS NMR, *o*-xylene and 1,2,4-trimethylbenzene, are not found in the products. This product exclusion places the effective catalytic pore size between 7.26 Å (MIN-2 of *m*-xylene, Table 1) and 7.27 Å (MIN-2 of *o*-xylene, Table 1). This fine resolution of the effective catalytic pore size is an artifact of the data because the *m*- and *p*-xylene are reported together. The effective

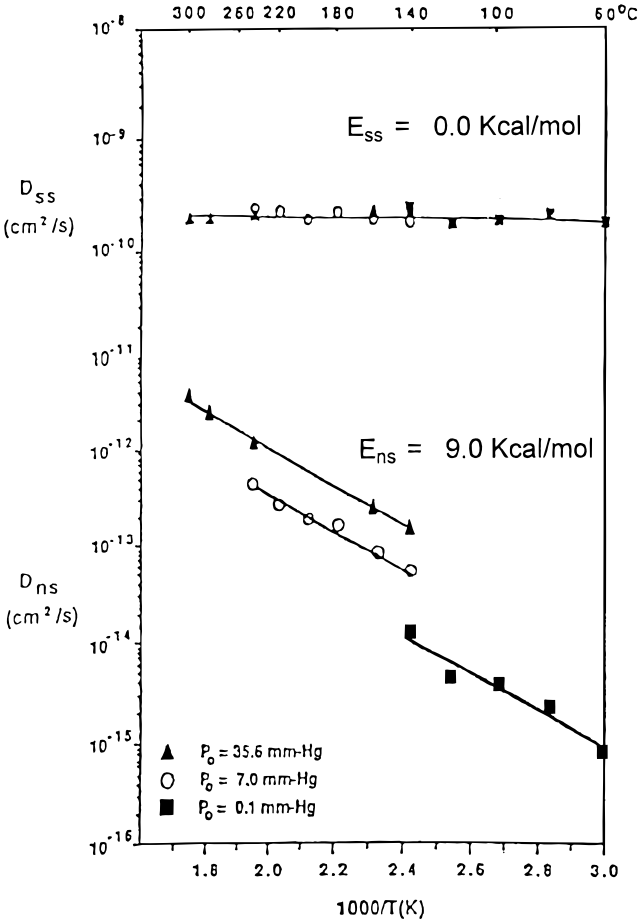

Figure 5. Determination of the activation energy for steady-state diffusivity (E_{ss}) and uptake diffusivity (E_{ns}) at various pressures over a given temperature range. A uniform value of the steady-state diffusivity is attained for all cases of pressure and temperature. A steady-state diffusion activation energy (E_{ss}) of 0.0 kcal/mol requires that *o*-xylene (MIN-2 of 7.27 Å) be able to "freely diffuse" through the HZSM-5 structure. The steady-state diffusion activation energy for *p*-xylene (MIN-2 of 6.62 Å) and 2-methylnaphthalene (MIN-2 of 7.35 Å) also have $E_{ss} = 0.0$ kcal/mol. After ref 31.

catalytic pore size is better realized as being between 6.62 Å (MIN-2 of *p*-xylene, Table 1) and 7.27 Å (MTN-2 of *o*-xylene, Table 1). These results are consistent with a previous study[28] which finds that neither channel is accessible to 2,6-di-*tert*-butylpyridine (MIN-2 of 8.29, Table 1) at 25 °C. It should be noted that preferential-diffusion product selectivity can be induced by increasing the liquid hourly space velocity (LHSV [flow rate]) of the feed stock through the reaction apparatus over the catalyst bed.

At 370 °C, the product stream of the HZSM-5 catalyzed conversion of methanol to gasoline contains aromatic molecules no larger than 1,2,3-trimethylbenzene (Table 2). This reaction product requires the effective catalytic pore size to be at least 7.64 Å (Table 1). 1,2,4-trimethylbenzene is the next smaller isomer and is therefore allowed to exit the structure. The possibility that 1,2,3-trimethylbenzene is a product of the isomerization of 1,2,4-trimethylbenzene from exterior surface activity is unlikely. The thermodynamically favored isomer is 1,3,5-trimethylbenzene, and the favored isomerization product is 1,2,3-trimethylbenzene by the nest effect. An isomerization of 1,2,4-trimethylbenzene would produce both of the other two isomers (favoring the 1,2,3-), but no 1,3,5-trimethylbenzene was observed. Although molecules ranging in size from 1,2,3,4-tetramethylbenzene to hexamethylbenzene (MIN-2 of 7.65 Å to MIN-2 to 9.08 Å, Table 1) are in the adsorbed phase, they do not show up in the product stream. More temperature studies on this catalytic reaction would be required to ascertain an exact temperature at which the larger molecules would not be selected against in the product stream (overcoming an activation energy for diffusion), but these studies could be complicated by surface activity isomerization.

The channel intersection allows for the formation of molecules greater in size than 1,2,4-trimethylbenzene at 300 °C and larger than 1,2,3-trimethylbenzene at 370 °C. At 300 °C, the largest molecule formed at the intersection is 1,2,3,5-tetramethylbenzene (MIN-2 of 8.17 Å by MIN-2 of 8.88 Å). At 370 °C, the intersection allows for the formation of molecules as large as pentamethylbenzene and hexamethylbenzene. This formation of larger sized products at 370 °C indicates an increase in the apparent size of the intersection from 8.17 Å by 8.88 Å to at least 9.08 Å by 9.09 Å (MIN-2 by MIN-3 for hexamethylbenzene).

Fraenkel and Levy concluded that neither pentamethyl- nor hexamethylbenzene are found in the product stream of the methanol conversion catalyzed by HZSM-5[27a] at reaction conditions similar to those of Chang and Silvestri.[29] Fraenkel and Levy do not report production of 1,3,5-trimethylbenzene, 1,2,3,4-tetramethyl-, or 1,2,3,5-tetramethylbenzene.[27a] The crystal size of the HZSM-5 catalyst used in the investigation was between 5 and 10 μm.[27b] Along with the crystal size of the catalyst, the absence of the third trimethylbenzene isomer as well as the other two tetramethylbenzene isomers leads to the conclusion that the exterior surface activity of the particular HZSM-5 catalyst was minimal.

At the proper conditions, the selectivity of the MTG process (with "equilibrium MTG catalyst") is essentially exclusive to the 1,2,4-trimethylbenzene isomer (over the two other trimethyl isomers) and to the 1,2,4,5-tetramethylbenzene (over the two other tetramethyl isomers).[30] The MTG process uses HZSM-5 crystals which are of submicron size.[30] Such particles would be expected to have a large ratio of exterior surface activity compared to larger crystals (>1 micron). It should be noted that, if present, exterior surface acidity of the zeolite could isomerize the alkyl-substituted benzenes to near equilibrium distributions. As a catalytic reaction progresses, if present, the surface activity is quenched, and slight coking of the pore structure could lead to greater selectivity based on size.

A previous study[28] reported that the sinusoidal (small) channel of HZSM-5 contains the strong Brønsted acid site. It is reported that small channel acid site is accessed by pyridine (MIN-2 of 6.48 Å) but not by 2,6-lutidine (MIN-2 of 6.96 Å) at 25 °C. This would set the difference in the effective catalytic pore size of the two channels at room temperature to be no greater than 0.48 Å. One should not conclude that the catalytic formation of aromatic compounds in the conversion of methanol to gasoline must always occur at the strongest Brønsted site because the dimensions of the largest formed molecules are larger than allowed in either of the channels (when formed inside the structure opposed to formed on the exterior of the structure).

Product Selectivity. While the product distribution of the xylenes at 300 °C demonstrates preferential-diffusion product selectivity, this distribution is not the only evidence. The activation energy of diffusion for a probe molecule in a given structure reflects the extent of interaction of the probe with the walls of the structure itself. If the probe molecule can freely diffuse without hindrance (repulsion) from the structure, the activation energy for diffusion is zero. Since the non-steady-state (apparent) diffusivity of a probe molecule reflects ther-

TABLE 2: Distribution of Aromatics in the Product Stream and in the Adsorbed Phase from Methanol Conversion over HZSM-5

				product stream by gas chromatography				adsorbed-phase by ^{13}C MAS NMR[10]	
		distribution		300 °C[12]		370 °C[27a]			
compound	MIN-2 (Å)	statistical[a]	thermodynamic[b]	distribution (%)[c]	wt %[d]	distribution (%)[c]	wt %[e]	300 °C[f]	370 °C[f]
benzene	6.63						1.0		w
toluene	6.63						11.6	w	m
xylenes									
p-	6.62	10.0%	23.5%	100%[g]	1.6[g]	38.5%	21.1	s	m
m-	7.26	40.0%	52.7%			43.5%	23.8	w	s
o-	7.27	40.0%	23.8%	0%	0	18.0%	9.9	s	s
trimethylbenzenes									
1,2,4-	7.25	63.2%	66.0%			93.5%	20.1	m	m
1,2,3-	7.64	26.3%	7.8%			6.5%	1.4	w	m
1,3,5-	8.18	10.5%	26.2%			0.0%	0.0	w	w
tetramethylbenzenes									
1,2,4,5-	7.38	10.0%	33.4%			100%	1.0	s	w
1,2,3,4-	7.65	40.0%	16.0%			0.0%	0.0	w	vw
1,2,3,5-	8.17 × 8.88[h]	40.0%	50.6%			0.0%	0.0	m	vw
pentamethylbenzene	8.22 × 9.09[h]								w
hexamethylbenzene	9.08 × 9.09[h]								w

[a] Expected for random methyl substitution on the benzene ring. [b] Thermodynamic equilibrium distributions at 371 °C.[29] Values for the xylenes at 300 °C are *p*:*m*:*o*::24.1%:54.4%:21.5%.[35] [c] Normalized isomer distribution. [d] Weight percent of (total normalized, hydrocarbon) product stream. 1.24 LHSV (liquid hourly space velocity), 45 min TOS (time on stream), 82.4% COM (conversion of methanol), aromatics were 9.2 wt % of hydrocarbon products. [e] Weight percent of (normalized, total collected organic liquid) product stream. 1.5 WHSV (weight hourly space velocity), 105 min TOS, 100% COM. The organic liquid does not contain the lighter hydrocarbons (smaller than pentane and with some pentane loss). Aromatics were 86.5 wt % of collected organic liquid products. [f] s = strong, m = medium, w = weak, and vw = very weak intensity. TOS of 35 min for 300 °C and 33 min for 370 °C. [g] *m*- and *p*-xylene were reported together, not individually. [h] The second quoted dimension is MIN-3.

TABLE 3: Comparison of Space Velocity Effects on Distribution of Xylenes in the Product Stream from Methanol Conversion over HZSM-5 at 300 °C

			product stream by gas chromatography[12]							
			LHSV[b] = 0.15[c]		LHSV = 0.31[d]		LHSV = 0.62[e]		LHSV = 1.24[f]	
compound	MIN-2 (Å)	thermodynamic distribution[a]	distribution (%)[g]	wt %[h]	distribution (%)[g]	wt %[h]	distribution (%)[g]	wt %[h]	distribution (%)[g]	wt %[h]
xylenes										
p-	6.62	24.1%	78.9%[i]	7.1[i]	87.9%[i]	9.4[i]	93.2%[i]	4.1[i]	100%[i]	1.6[i]
m-	7.26	54.4%								
o-	7.27	21.5%	21.1%	1.9	12.1%	1.3	6.8%	0.3	0%	0.0
trimethylbenzene										
1,2,4-	7.25	67.7%	100%	4.5	100%	4.0	100%	2.6	0%	0.0

[a] Thermodynamic equilibrium distributions at 300 °C.[35] [b] LHSV (liquid hourly space velocity [mL hr^{-1}]). [c] 45 min TOS (time on stream), 100% COM (conversion of methanol), aromatics were 16.9 wt % of HP (hydrocarbon products). Xylenes were 53.2% of AP (aromatic products). [d] 45 min TOS, 100% COM, aromatics were 21.9 wt % of HP. Xylenes were 48.8% of AP. [e] 45 min TOS, 90.5% COM, aromatics were 9.2 wt % of HP. Xylenes were 47.8% of AP. [f] 45 min TOS, 82.4% COM, aromatics were 1.6 wt % of HP. Xylenes were 100% of AP. [g] Normalized isomer distribution. [h] Weight percent of (total normalized, hydrocarbon) product stream. [i] *m*- and *p*-xylene were reported together, not individually.

modynamic properties in addition to characteristics of the stochastic process, the temperature dependence of the steady-state diffusivities must be determined in order to examine if the diffusing molecule experiences any repulsion with the framework structure. The observation that the steady-state diffusivity (D_{ss}) of *o*-xylene in HZSM-5 has an activation energy of 0.0 kcal/mol[31] explicitly states that an *o*-xylene molecule does not experience any repulsions from the framework structure of HZSM-5 (Figure 5). This D_{ss} was determined over a wide range of temperatures (60 to 315 °C) and loadings (pressures), and this result can be extended to the other molecules of lesser size in the HZSM-5 structure. In this same study,[31] consistent with the findings for *o*-xylene, the steady-state diffusivity determined activation energy of *p*-xylene (smaller than *o*-xylene, MIN-2 of 6.62 Å) and 2-methylnaphthalene (slightly larger than *o*-xylene, MIN-2 of 7.35 Å) were also found to be 0.0 kcal/mol. As expected, although *p*-xylene has 0.0 kcal/mol activation energy for diffusion, it still diffuses at a much higher rate than does the larger *o*-xylene molecule.

Preferential-diffusion product selectivity may also be achieved with the increase of the flow velocity (e.g., LHSV) of the reactant feedstock through the catalyst bed.[12] While the conversion of the reactant feed is decreased and the selectivity to aromatics products is decreased, the products with smaller minimum dimensions will be favored (Table 3). It should be noted that at the slowest flow rate, the xylene isomer distribution is essentially that of the thermodynamic distribution at the same temperature. This correspondence of the distributions is expected because the stochastic contribution to the product distribution is removed at low space velocities.

Various investigators have demonstrated size-exclusion product selectivity, simply by digesting spent catalyst and determining the reaction products not allowed to exit the structure.[32] Large molecules (biphenyls, alkylnaphthalenes, etc.) are among the retained residue from the catalyzed reaction of benzene and toluene.

Nest Effect. In the HZSM-5 catalyzed conversion of methanol to gasoline over small crystal catalyst, the distribution of the poly-substituted methylbenzenes in the product stream should be the same as that of a nonselective catalyst (the thermodynamic distribution) if no nest effect is present. The smallest isomer would be produced, and in the case of a nest effect (by

TABLE 4: Distribution of Aromatics in the Product Stream from Methanol Conversion over Small Crystal HZSM-5 at 371 °C

compound	MIN-2 (Å)	thermodynamic product distribution[a]	product stream by gas chromatography[29] distribution (%)[b]	product stream by gas chromatography[29] wt %[c]
benzene	6.63			1.7
toluene	6.63			10.5
xylenes				
p-	6.62	23.5%	23.9%	4.09
m-	7.26	52.7%	54.6%	9.06
o-	7.27	23.8%	21.5%	4.04
trimethylbenzenes				
1,2,4-	7.25	66.0%	78.7%	4.57
1,2,3-	7.64	7.8%	6.4%	0.37
1,3,5-	8.18	26.2%	14.9%	0.87
tetramethylbenzenes				
1,2,4,5-	7.38	33.4%	46.5%	0.82
1,2,3,4-	7.65	16.0%	9.3%[d]	0.16
1,2,3,5-	8.17 × 8.88[e]	50.6%	44.2%	0.78
pentamethylbenzene	8.22 × 9.09[e]			<0.2[f]

[a] Thermodynamic equilibrium distributions at 371 °C.[29] [b] Normalized isomer distribution. [c] Weight percent of (total normalized, hydrocarbon) product stream. 1.0 LHSV (liquid hourly space velocity), 60 min TOS[30] (time on stream); 100% COM (conversion of methanol), aromatics were 41.2 wt % of hydrocarbon products. [d] Reported incorrectly in ref 29. [e] The second quoted dimension is MIN-3. [f] 0.2 wt % of the (total normalized, hydrocarbon) product stream was C_{11}^+. Only trace amounts of pentamethylbenzene are found, and it is not possible to either quantify or pinpoint its origin.[30]

isomerization), would produce the other isomers, with the less steric attack selected over the more steric.

Chang concluded that trace amounts of pentamethylbenzene can be found in the product stream of the MTG process at the proper conditions (e.g., elevated temperatures, etc.), but that "it is not possible either to quantify or pinpoint [pentamethylbenzene's] origin".[30] The question arises as to the source of the pentamethylbenzene. Exterior surface activity of the zeolite can isomerize and even methylate substituted benzenes. Chang believes that "if [one] looked hard enough, [one] could even find hexamethylbenzene".[30] The crystallite size of HZSM-5 used in studies of Chang and Silvestri[29] was <0.05 micron.[30]

Chen reports that surface activity can be neglected when the crystal size is greater than 1 micron because the external surface area relative to the intracrystalline surface area is less than one percent.[33] "One should exercise caution in assuming that external surface sites can be neglected with large crystals of ZSM-5. All things being equal, this might be true; however, many preparations of large crystal material tend to exhibit Al zoning (gradient), i.e., a higher concentration of Al at or near the crystal surface (von Ballmoos, R.; Meier, W. M. *Nature* **1981**, *289*, 782), thus actually increasing external site density".[30]

For the xylenes at 371 °C in the methanol conversion over HZSM-5, the largest isomer (*o*-xylene) is decreased from its thermodynamic equilibrium amount, while the two smaller isomers (*m*- and *p*-xylene) are increased. For the trimethylbenzenes at 371 °C, the largest isomers (1,2,3- and 1,3,5-trimethylbenzene) are decreased from their thermodynamic equilibrium amount, while the smallest isomer (1,2,4-trimethylbenzene) is increased. For the tetramethylbenzenes at 371 °C, again the two largest isomers (1,2,3,5-tetramethylbenzene and 1,2,3,4-tetramethylbenzene) are decreased, while the smallest isomer (1,2,4,5-tetramethylbenzene) is increased from its thermodynamic equilibrium amount (See Table 4).

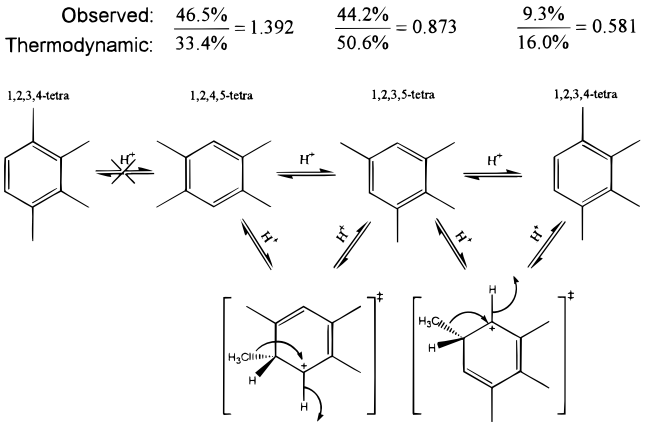

Figure 6. Illustration of the isomerization of 1,2,4,5-tetramethylbenzene. While the isomerization of 1,2,4,5-tetramethylbenzene to 1,2,3,5-tetramethylbenzene may occur by a one-step process (1,2-methyl shift), the 1,2,4,5- cannot directly isomerize to the 1,2,3,4-tetramethylbenzene. However, the 1,2,3,5-tetramethylbenzene can isomerize directly to the 1,2,4,5-tetramethylbenzene.

The distributions of the isomers of the polysubstituted methylbenzenes represent the nest effect from the activity of the exterior surface of the HZSM-5 catalyst. One should consider the results of the 371 °C reaction catalyzed with small crystal HZSM-5 interesting from the point that the final distribution of dimethyl-substituted products is close to the thermodynamic distribution, but slightly favors the nonsteric product (*m*-xylene favored over *o*-xylene, see Table 4).

The nest effect could be indicated by the ratio of the isomeric distributions of the tetramethylbenzenes (see Table 4 and Figure 6). The exterior surface shape selectivity would isomerize 1,2,4,5-tetramethylbenzene selecting towards the less steric isomer (of the two larger isomers). Since the production of 1,2,3,4-tetramethylbenzene by the isomerization of 1,2,4,5-tetramethylbenzene would have to occur via a 1,3-methyl shift, the 1,2,3,4-tetramethylbenzene cannot be produced in one direct step. The production of 1,2,3,4-tetramethylbenzene must come from a 1,2-methyl shift of the 1,2,3,5-tetramethylbenzene, which was produced by a 1,2-methyl shift of 1,2,4,5-tetramethylbenzene (Figure 6). Therefore, the tetramethylbenzene isomeric group can not give direct experimental observation of the exterior surface activity's shape selectivity (nest effect).

The trimethylbenzene isomeric group can give a direct experimental observation of the exterior surface activity's shape selectivity because the isomerization of 1,2,4-trimethylbenzene could produce either the 1,2,3-trimethylbenzene isomer or the 1,3,5-trimethylbenzene isomer via a 1,2-methyl shift (Figure 7). Since either isomer can be produced independent from the other, the ratio of each isomer's observed value compared with its thermodynamic equilibrium value demonstrates a selectivity towards the less steric attack (1,2,3-trimethyl isomer), even though this isomer is thermodynamically unfavored compared to the 1,3,5-trimethyl isomer (Table 4).

Conclusions

The temperature dependent effective catalytic pore size of HZSM-5 is concluded to be between 6.62 Å (MIN-2 of *p*-xylene) and 7.27 Å (MIN-2 of *o*-xylene) at 300 °C. The effective pore size is increased to a minimum of 7.64 Å (MIN-2 of 1,2,3-trimethylbenzene) at 370 °C. The increase in temperature effectively increases the channel intersection from 8.17 Å by 8.88 Å to 9.08 Å by 9.09 Å.

Minimum dimensions (MIN-1 and MIN-2) are a scale of particle size based on calculations using geometries obtained

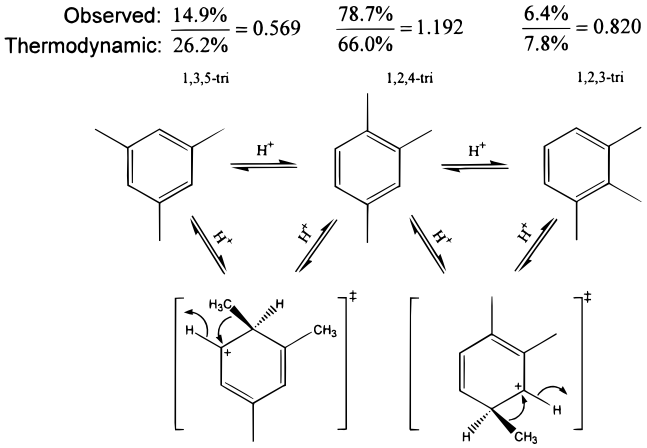

Figure 7. Illustration of the isomerization of 1,2,4-trimethylbenzene. The isomerization of 1,2,4-trimethylbenzene can occur directly to either the 1,2,3- or 1,3,5-trimethylbenzene through a 1,2-methyl shift. The nest effect can be directly observed by comparing the ratios of the observed to thermodynamic distributions of 1,2,3- and 1,3,5-trimethylbenzene. Even though the isomerization thermodynamically favors 1,3,5-trimethylbenzene, the 1,2,3-trimethylbenzene has a higher ratio of observed product.

from quantum chemistry, and volumes and projected dimensions calculated from these geometries using our model. This model yields dimensions that are reasonable, that are uniquely defined, and that are not inconsistent with molar volumes, for example. All of the calculated dimensions suggest these molecules are too big to fit in the pores suggested from the static structures of the zeolites. Nevertheless, we have generated a very reasonable, first principles, measurement of relative sizes, although this particular choice of calculation is, admittedly, arbitrary. We have then calibrated the effective size of the pore using a combination of experiment and our calculated results, and this is independent of the real or imagined pore size of the zeolite.

When one uses the van der Waals radii of oxygen or the oxide ion radius to calculate a window size of the large channel of HZSM-5 (or their LJ corrected radii), neither produce a pore of the necessary dimensions to allow for the entry or exit of these large aromatic molecules. These calculated window sizes do not allow for the nonrestricted diffusion of *o*-xylene, demonstrated by the 0.0 kcal/mol activation energy for steady-state diffusion.

The distribution of the polysubstituted methylbenzenes in the product stream of the HZSM-5 catalyzed conversion of methanol to gasoline are what one would expect, the largest isomer of each group is selected against (Table 2). For the xylenes at 300 °C, the largest isomer (*o*-xylene) is completely selected against, while the amounts of the two smaller isomers (*m*- and *p*-xylene) are increased from that expected from thermodynamic equilibrium. For the xylenes at 370 °C, the amount of the largest isomer (*o*-xylene) is decreased from that expected at thermodynamic equilibrium, while the two smaller isomers (*m*- and *p*-xylene) are increased. At 300 °C, the trimethylbenzenes and tetramethylbenzenes are entirely selected against. For the trimethylbenzenes at 370 °C, the largest isomer (1,3,5-trimethylbenzene) is entirely selected against, the middle-sized isomer is decreased from its thermodynamic equilibrium, and the smallest isomer (1,2,4-trimethylbenzene) is highly favored. For the tetramethylbenzenes at 370 °C, the two largest isomers (1,2,3,5-tetramethylbenzene and 1,2,3,4-tetramethylbenzene) are completely selected against, while the smallest isomer (1,2,4,5-tetramethylbenzene) is favored and is thus increased from its thermodynamic equilibrium amount.

The nest effect (shape selectivity of the exterior surface activity of the zeolite) has been demonstrated by the distribution of the trimethylbenzene isomers produced from the conversion of methanol (and isomerization of 1,2,4-trimethylbenzene) over small crystal HZSM-5 (Table 4). Since either isomer can be produced independent from the other (Figure 7), a comparison of the ratio of the trimethylbenzene isomer's observed value with its thermodynamic equilibrium value demonstrates selectivity towards the less steric attack (1,2,3-trimethylbenzene), even though the 1,3,5-trimethyl isomer is thermodynamically favored.

The species found in the adsorbed phase reaction products demonstrate the second type of product selectivity, size-exclusion. The adsorbed phase contains molecules that cannot diffuse though either channel of the zeolite. This type of pore-confinement product selectivity excludes the reaction product from the product stream, contrary to the classically described, preferential-diffusion product selectivity, which allows for diffusion of all reaction products.

While limited selectivity towards *p*-xylene (two-fold increase in distribution compared to thermodynamic equilibrium) over *o*- and *m*-xylene is achieved by HZSM-5 in the methanol alkylation of toluene,[34] increased selectivity for *p*-xylene (>97%) can be attained by modified ZSM-5.[34] Increased flow rates over HZSM-5 can increase selectivity towards the elongated products (i.e., *p*-xylene, see Table 3).[12] These results, as well as the 0.0 kcal/mol activation energy for the steady-state diffusion of *o*-xylene, show that the often cited, preferred alkylation of toluene to *p*-xylene over HZSM-5[7] is governed by the retarded diffusion of the other two larger isomers (*o*- and *m*-). Therefore, this selectivity is from purely kinetic considerations—kinetic transport (i.e., increased diffusivity) of *p*-xylene is the reason for the increased selectivity over HZSM-5.

The discussion of dimensions for the determination of actual pore sizes should be put in perspective. The dimensions one chooses are quite arbitrary; it is the consistency with which measurements are determined which is important. Since crystallographic derived pore sizes are well below those expected from experimentally derived chemical correlations and the portability of probe based measurements are more convenient for comparison of different structures, this method for determining the temperature dependent, effective catalytic pore size has worked well with this HZSM-5-catalyzed methanol conversion and has great potential for further study.

Acknowledgment. The authors thank the Environmental Protection Agency (EPA), the National Science Foundation (NSF Grant CHE9726689), Edgewood Research, Development, and Engineering Center (ERDEC), the Army Research Office (ARO), and the Office of Naval Research (ONR) for financial support as well as additional funding from an IBM SUR Grant. The authors acknowledge very helpful discussions with Dr. Clarence D. Chang of the Mobil Corporation. His input was invaluable. The authors also acknowledge Dr. Paul B. Weisz for the permission to include his figure as our Figure 5.

References and Notes

(1) Chang, C. D. *Hydrocarbons from Methanol*; Marcel Dekker, Inc.: New York, 1983. Chen, N. Y.; Degnan, T. F., Jr.; Smith, C. M. *Molecular Transport and Reaction in Zeolites*; VCH Publishers: New York, 1994.

(2) Barrer, R. M. *Zeolites and Clay Minerals as Sorbents and Molecular Sieves*; Academic Press: London, 1978. Breck, D. W. *Zeolite Molecular Sieves*; John Wiley & Sons: New York, 1974. Dyer, A. *An Introduction to Zeolite Molecular Sieves*; John Wiley & Sons: New York, 1988. Rabo, J.

A. *Zeolite Chemistry and Catalysis*, *ACS Monograph 171*; American Chemical Society: Washington, DC, 1976.

(3) Davis, M. E.; Suib, S. L. *Selectivity in Catalysis*; ACS Symposium Series 517; American Chemical Society: Washington, DC, 1993.

(4) Dyer, A. *An Introduction to Zeolite Molecular Sieves*; John Wiley & Sons: New York, 1988; p 117.

(5) Chen, N. Y.; Degnan, T. F., Jr.; Smith, C. M. *Molecular Transport and Reaction in Zeolites*; VCH Publishers: New York, 1994; p 174.

(6) Davis, M. E.; Suib, S. L. *Selectivity in Catalysis*; ACS Symposium Series 517; American Chemical Society: Washington, DC, 1993; p 209.

(7) Csicery, S. M. *Chem. Br.* **1985**, *May*, 473.

(8) Davis, M. E.; Suib, S. L. *Selectivity in Catalysis*; ACS Symposium Series 517; American Chemical Society: Washington, DC, 1993; pp 210−211.

(9) Chen, N. Y.; Degnan, T. F., Jr.; Smith, C. M. *Molecular Transport and Reaction in Zeolites*; VCH Publishers: New York, 1994; p 182.

(10) Anderson, M. W.; Klinowski, J. *J. Am. Chem. Soc.* **1990**, *112*, 10−16. Anderson, M. W.; Klinowski, J. *Nature* **1989**, *339*, 200−203.

(11) Olson, D. H.; Kokotailo, G. T.; Lawton, S. L. *J. Phys. Chem.* **1981**, *85*, 2238−2243.

(12) Derouane, E. G., Nagy, J. B., Dejaifve, P., van Hoof, J. H. C.; Spekman, B. P.; Vedrine, J. C.; Naccache, C. *J. Catal.* **1978**, *53*, 40−55.

(13) Dyer, A. *An Introduction to Zeolite Molecular Sieves*; John Wiley & Sons: New York; 1988; pp 97−98.

(14) Chen, N. Y.; Degnan, T. F., Jr.; Smith, C. M. *Molecular Transport and Reaction in Zeolites*; VCH Publishers: New York, 1994; p 132.

(15) Csicsery, S. M. *J. Catal.* **1971**, *23*, 124.

(16) Murakami, Y.; Iijima, A.; Ward, J. W. *New Developments in Zeolite Science and Technology*; Elsevier: New York, 1986; pp 669−675.

(17) Young, D. M.; Crowell, A. D. *Physical Adsorption of Gases*; Butterworths: London, 1962; p 19.

(18) Derouane, E. G. *J. Catal.* **1986**, *100*, 541. Derouane, E. G.; Andre, J. M.; Lucas, A. A. *J. Catal.* **1988**, *110*, 58.

(19) Chen, N. Y.; Degnan, T. F., Jr.; Smith, C. M. *Molecular Transport and Reaction in Zeolites*; VCH Publishers: New York, 1994; p 189.

(20) Zerner, M. C. and co-workers. ZINDO; Department of Chemistry, University of Florida, Gainesville, FL 32611. Zerner, M. C. *Reviews of Computational Chemistry*, VCH Publishing: New York, 1991; Vol. 2, pp 313−366.

(21) For GEPOL93, see: Pascual-Ahuir, J. C.; Silla, E.; Tunon, I.; Silla, E.; Tunon, I.; Pascual-Ahuir, J. C. *J. Comput. Chem.* **1991**, *12*, 1077.

(22) Chen, N. Y.; Degnan, T. F., Jr.; Smith, C. M. *Molecular Transport and Reaction in Zeolites*; VCH Publishers: New York, 1994; p 133.

(23) The values used for the center-to-center oxygen distances were obtained from the fractional coordinates of the van Koningsveld et al. paper,[24] which had improved framework accuracy over previous reports. The oxygen atoms used were those of Olson et al.,[11] the largest (8.449 Å) and smallest (7.922 Å) center-to-center oxygen atom distances for the straight channel.

(24) van Koningsveld, H.; van Bekkum, H.; Jansen, J. C. *Acta. Crystallogr.* **1987**, *B43*, 127−132.

(25) Dean, John A. *Lange's Handbook of Chemistry*, 14th ed.; McGraw-Hill, Inc: New York, 1992; p 4·18. Emsley, J. *The Elements*; Oxford University Press, Inc.: New York, 1991; p 136.

(26) Webster, C. E.; Drago, R. S.; Zerner, M. C. *J. Am. Chem. Soc.* **1998**, *120*, 5509−5516.

(27) (a) Fraenkel, D.; Levy, M. *J. Catal.* **1989**, *118*, 487−493. (b) Fraenkel, D.; Levy, M. *J. Catal.* **1989**, *118*, 10−21.

(28) Drago, R. S.; Diaz, S.; Torrealba, M.; de Lima, L. *J. Am. Chem. Soc.* **1997**, *119*, 4444−4452.

(29) Chang, C. D.; Silvestri, A. J. *J. Catal.* **1977**, *47*, 249−259.

(30)) Chang, C. D. Personal Communication.

(31)) Weisz, P. B. *Ind. Eng. Chem. Res.* **1995**, *34*, 2692−2699.

(32) Anderson, J. R.; Dong, Q. N.; Chang, Y. F.; Western, R. J. *J. Catal.* **1991**, *127*, 113−127. Anderson, J. R.; Chang, Y. F.; Western, R. J. *J. Catal.* **1989**, *118*, 466.

(33) Chen, N. Y.; Degnan, T. F., Jr.; Smith, C. M. *Molecular Transport and Reaction in Zeolites*; VCH Publishers: New York, 1994; p 189.

(34) Chen, N. Y.; Kaeding, W. W.; Dwyer, F. G. *J. Am. Chem. Soc.* **1979**, *101*, 6783−4.

(35) Hastings, S. H.; Nicholson, D. E. *J. Chem. Eng. Data* **1961**, *6*, 1−4.